Blanco-Cano, L., Soria-Verdugo, A., Garcia-Gutierrez, L. M., & Ruiz-Rivas, U. (2016). Modeling the thin-layer drying process of granny smith apples: Application in an indirect solar dryer. *Applied Thermal Engineering*, 108, 1086-1094

DOI: https://doi.org/10.1016/j.applthermaleng.2016.08.001

Modeling the thin-layer drying process of Granny Smith apples: Application in an indirect solar dryer.

L. Blanco-Cano[a], A. Soria-Verdugo[b*], L.M. Garcia-Gutierrez[b], U. Ruiz-Rivas[a,b]
a: Appropriate Technology Group b: Energy Systems Engineering
*: corresponding author: asoria@ing.uc3m.es
Department of Thermal and Fluids Engineering. University Carlos III of Madrid.
Avda. Universidad 30, 28911, Leganés (Spain). Tel. +34916248465

Abstract

The thin-layer drying kinetics of Granny Smith apples is determined by thermogravimetric analysis of the drying process at constant temperatures ranging from 20 °C to 50 °C, using intervals of 5 °C. The experimental drying curves obtained in the TGA were fitted to the Wang-Singh equation, which was found to describe precisely the drying process. A novel model, capable of predicting the evolution of the moisture ratio of Granny Smith apples during the drying process and under variable drying temperatures, was proposed. The model was validated with experimental TGA measurements of the drying of apples at variable temperatures, typical of solar drying, obtaining maximum deviations for the drying time of less than 1.5%. Once validated, the model proposed was also applied to the drying of Granny Smith apples in an indirect solar dryer. The comparison of the model prediction with the experimental measurements of the drying of apples at variable drying conditions conducted in a lab-scale solar dryer showed a proper agreement, with low deviations (less than 10%) due to the thermal inertia of the samples.

Keywords

Solar drying; Granny Smith apples; Drying kinetics; Thin-layer drying; TGA; Mathematical model.

1. Introduction

Solar drying is a commonly used method for preservation or processing of a wide variety of agricultural products [1-3]. Apples are selected in this work as test products since they are an important raw material produced all around the world. Dried apples can be consumed directly or treated as a secondary raw material [4]. The variety of apples named Granny Smith is characterized by growing in areas with climates relatively warm [5] which makes this variety suitable for solar drying. Solar drying of different varieties of apples has been analyzed in the literature [6-8], but no experiences on Granny Smith have been found.

In indirect solar dryers, the drying process depends mainly on the drying conditions (air mass flow rate, and airflow temperature and relative humidity) in the drying chamber and on the drying kinetics of the product at those conditions. The drying conditions at the inlet of the drying chamber depend on the air heating process in the solar collector [9], and thus the drying process is highly dependent on the ambient conditions and the solar irradiance. While the solar drying process is characterized by variable drying conditions, the drying kinetics is generally studied at constant drying conditions.

The thin-layer drying is the procedure of drying one single layer of particles or slices of a product. The thin-layer equations predict the temporal evolution of the moisture content of the samples, based on empirical models of the drying process: Lewis, Page, Henderson and Pabis, Logarithmic, two terms, two terms exponential, Wang and Singh, among others [10]. These models have been widely used in the study of the drying kinetics or to obtain the diffusion coefficient of several agricultural products [3, 11-15]. When the drying kinetics obtained at constant drying conditions are applied to the prediction of the evolution of a solar drying process, it is generally performed by means of mathematical simulation of the heat and mass transfer processes in the drying chamber [16, 17], which are simulations of high complexity. To the knowledge of the authors, there are no simple models available in the literature to predict the evolution of the moisture loss during the drying process at the variable drying conditions characteristic of solar drying processes.

Regarding the drying kinetics of apples, most of the works reported consist of the mathematical modeling of the drying curves obtained experimentally, employing the thin-layer equations at constant drying conditions, for different varieties of apples. The tests are typically conducted at different values of constant temperatures, and for different values of a second parameter, such as the sample thickness [18], the air velocity [19] the air relative humidity [20] or the temperature of the product [21]. Only a few researchers have focused on the drying kinetics of Granny Smith apples. Vega-Gálvez et al. [5] and Velic et al. [22] studied the drying kinetics in a range of temperatures between 40 °C and 80 °C. Doymaz [12] and González-Fésler et al. [23] reported the effect of different pre-treatments on the drying kinetics of Granny Smith apples at 60 °C and 65 °C respectively. However, these studies do not cover the whole range of temperatures of small-scale solar drying, which for Granny Smith application would be lower.

In this work, thin-layer drying tests were conducted in a TGA for several constant drying temperatures, obtaining the drying curves for Granny Smith apples. Different thin-layer equations available in the literature were fitted to the experimental drying curves obtained in the TGA. Then, a mathematical model capable of predicting the sample mass loss under variable temperatures is proposed and validated using TGA experimental results and experimental measurements obtained in a lab-scale solar dryer.

2. Experimental Setup

The experiments were conducted employing two different systems: a TGA and a lab-scale indirect solar dryer operated at controlled conditions. The lab-scale solar dryer can operate at either constant conditions or at the variable conditions corresponding to different climates. A characteristic climate of the harvest season of Granny Smith apples has been established and used as inlet conditions during the experiments. For the tests, fresh Granny Smith apples were employed.

2.1. Determination of the ambient conditions

In order to reproduce the solar drying process of Granny Smith apples during the drying experiments, the climate of the harvest season of a region in Spain where Granny Smith apples are cultivated is selected as the reference climate. The apples are typically harvested in that

region between the end of September and the beginning of October [24]. Data of solar irradiance, temperature and relative humidity are available online [25]. In the indirect solar dryer, air at ambient temperature and relative humidity is heated in the solar collector and directed to the drying chamber. Hence, the characteristic parameters of the climate for indirect solar drying applications are: the temperature and the relative humidity of ambient air, and the solar irradiance.

The solar air collector is inclined an angle β. Hence, according to Duffie and Beckmann [26], the solar irradiance on the collector angle is:

$$I_T = I_b R_b + I_d \left(\frac{1+\cos\beta}{2} \right) + I \rho_g \left(\frac{1-\cos\beta}{2} \right) \quad (1)$$

where I_b and I_d are the beam and diffuse components of the solar irradiance, I, respectively. R_b is the ratio of beam irradiance on tilted surface to that on the horizontal plane, determined by trigonometric relations, and ρ_g is the ground reflectivity. Hence, the irradiance on the tilted surface, I_T, depends on the location of the air heater, the collector angle and the solar time. Typical flat-plate solar collectors comprise an absorber plate and a glass cover [27]. Due to the transmittance of the glass cover and the absorptance of the absorber plate, only a fraction of the solar irradiation incident on the solar collector is absorbed by the absorber plate. The solar irradiance absorbed by the absorber plate can be determined as [26]:

$$S = I_b R_b (\tau\alpha)_b + I_d (\tau\alpha)_d \left(\frac{1+\cos\beta}{2} \right) + I \rho_g (\tau\alpha)_g \left(\frac{1-\cos\beta}{2} \right) \quad (2)$$

where $(\tau\alpha)_b$, $(\tau\alpha)_d$ and $(\tau\alpha)_g$ are the effective transmittance-absorptance products, referred to the beam, diffuse and reflected components, respectively, which depends on the materials of the solar air heater.

The solar irradiance on the horizontal plane (I) in a typical sunny day of the harvest season in the location where the apples are harvested is presented in Figure 1 a) in solid line. The solar irradiance on the collector angle (I_T), shown in dashed-dotted line, is calculated for a collector angle $\beta = 20º$. The solar irradiance absorbed by the absorber plate (S) that would be obtained in a typical small-scale solar dryer is calculated for the typical materials used in solar drying applications, and depicted in Figure 1 a) in dashed line. The solar irradiance absorbed by the absorber plate can be determined approximately in this case as $S \sim 0.95 \cdot I$. The ambient air temperature (T_0) and relative humidity (ϕ_0) are shown in Figure 1 b). Since the solar dryer takes the air from the ambient, T_0 and ϕ_0 correspond to the air conditions at the inlet of the solar dryer.

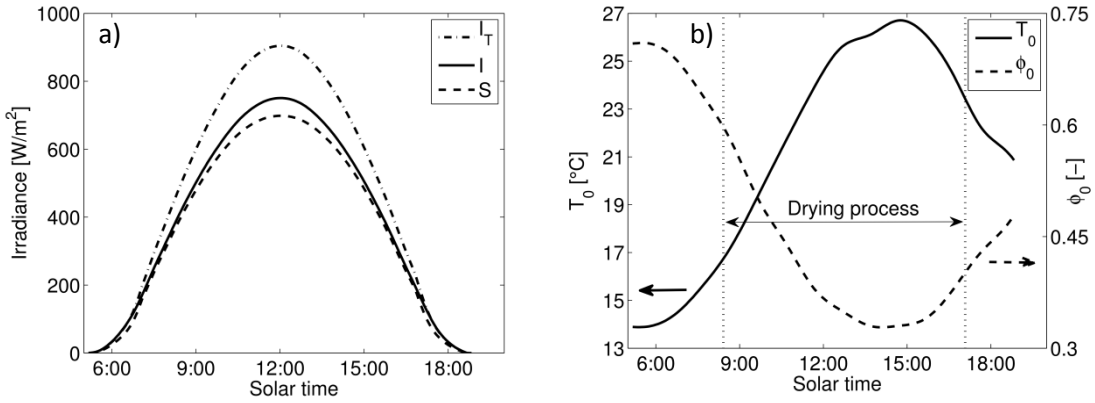

Figure 1: Characteristic parameters of the reference climate: a) solar irradiance on the collector angle, on the horizontal surface and absorbed by the absorber plate and b) temperature and relative humidity of the ambient air.

The ambient conditions shown in Figure 1 represent the reference climate to be simulated in the lab-scale solar dryer to reproduce the solar drying process of the Granny Smith apples. The drying process is considered to start when the relative humidity of the ambient air lowers 60% (which in this case occurs approximately 2.5 hours after the sunrise) and ends when the solar altitude angle lowers 10°.

2.2. Lab-scale indirect solar dryer and measurement system

A lab-scale indirect solar dryer was employed to reproduce the drying conditions on field. The experimental facility is composed of an air conditioning system to establish a prescribed airflow temperature and relative humidity, an artificial indirect solar dryer that reproduces the solar drying process, and the measurement and control systems. A schematic of the lab-scale indirect solar dryer is shown in Figure 2.

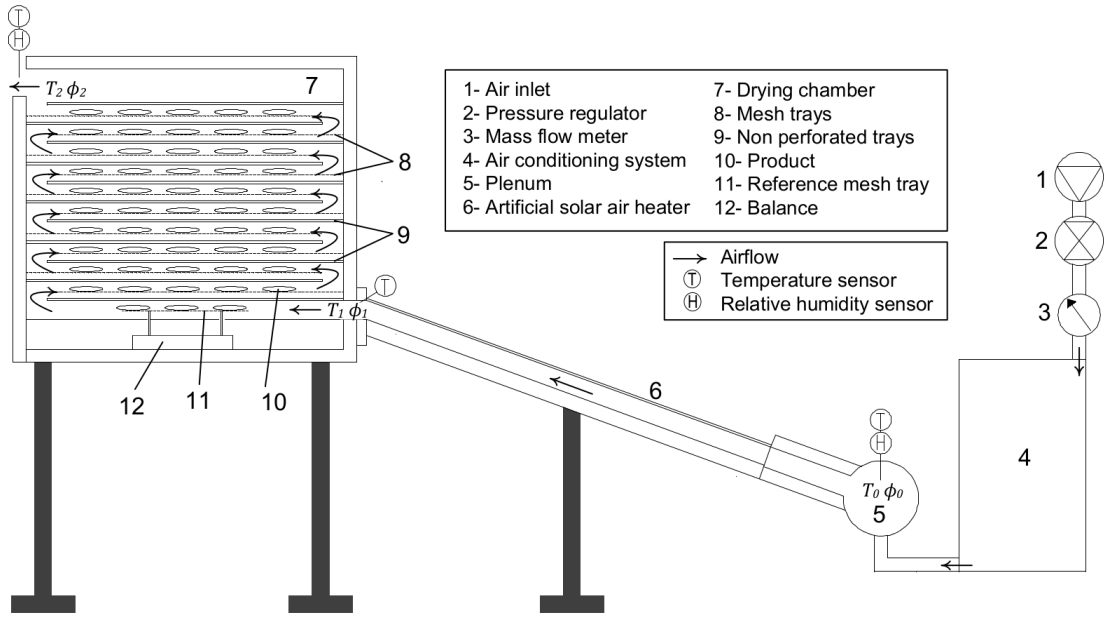

Figure 2: Schematic of the lab-scale indirect solar dryer.

The airflow is taken from the pneumatic air network (1) available in the laboratory. The air conditioning system (4) establishes the required air temperature (T_0) and relative humidity (ϕ_0) at the inlet of the solar collector. The airflow at temperature T_0 and relative humidity ϕ_0 is directed through the solar collector (6) to the drying chamber (7). An electrical resistance heats the airflow in the solar collector, supplying a variable thermal power equal to the product of the irradiance absorbed by the solar collector (S) times the collector area (A_C). The air enters the drying chamber at temperature T_1 and relative humidity ϕ_1. The drying chamber contains 13 non-perforated trays, arranged in series to maximize the airflow velocity around the product. The thin-layer samples of Granny Smith apples are located on wired mesh trays located between the non-perforated trays. The first tray lays on a balance that registers the sample mass variation each 5 s. Hence, the first mesh tray is used as the reference tray.

The solar dryer dimensions are presented in Table 1. These dimensions are within the typical range of small-scale indirect solar dryers. The walls and the bottom of the solar collector and the drying chamber are thermally isolated.

Table 1: Solar dryer dimensions.

Solar dryer component	**Dimension**
Collector length [m]	1
Collector width [m]	0.5
Distance between the absorber plate and the glass cover [m]	0.045
Drying chamber length [m]	0.75
Drying chamber width [m]	0.5
Drying chamber height [m]	0.64
Distance between trays [m]	0.045

The apples used for the tests are washed, cut into slices of 2.4 mm and immersed in citric acid to prevent oxidation [12]. The average total moisture content of the samples, determined for 25 samples dried in a Memmert UFE 500 oven, was 86.7%, with a standard deviation of 0.8%.

2.2.1. Measurement and control systems

The main characteristics of the measurement system are presented in Table 2, where the details of the location of the sensors, the type and the accuracy of the sensor used are reported. The air conditioning system and the power of the solar collector are controlled using a PID controller.

Table 2. Measurement system characteristics of the indirect solar dryer.

Measurement	**Location**	**Type of sensor**	**Accuracy**
Temperature of the airflow [ºC]	Inlet of the collector	NTC thermistor	± 0.3
	Outlet of the collector	T-type	± 1

		thermocouple	
	Outlet of the drying chamber	NTC thermistor	± 0.3
Relative humidity of the airflow [%]	Inlet of the collector	Capacitive sensor	1.5
	Outlet of the drying chamber		
Air mass flow rate [kg/s]	Inlet of the air conditioning system	Air mass flow meter SMC®	$9 \cdot 10^{-4}$
Mass of the product during the drying process [g]	Drying chamber. Reference tray	Balance PCE® 3 kg	1
Power of the electric heater of the solar collector [W]	AC supply	Power transducer	± 10

2.2.2. Drying Conditions

For the climate considered (Figure 1), and operating with an air mass flow rate of 0.015 kg/s in the lab-scale indirect solar dryer, the temperature and relative humidity of the airflow obtained at the inlet of the drying chamber (T_1 and ϕ_1) are presented in Figure 3. The drying conditions shown in Figure 3 will be employed during the drying process of Granny Smith apples at variable conditions in both the TGA and the indirect solar dryer tests.

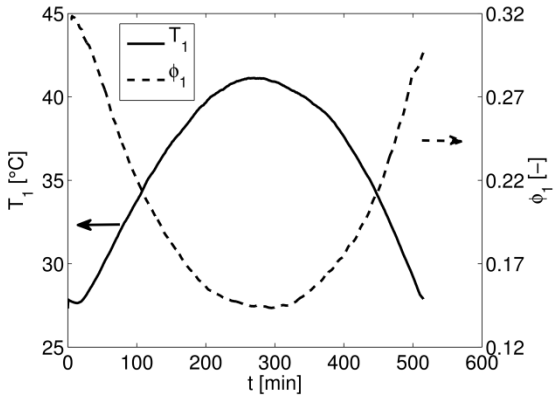

Figure 3: Temperature and relative humidity obtained at the inlet of the drying chamber.

The rate of solar energy used is determined by the collector efficiency, calculated as the ratio of useful heat absorbed by the airflow during the day to the total available solar irradiation. The collector efficiency during the drying process, considering the temperature T_1 depicted in Figure 3, the ambient temperature T_0 and the solar irradiance on the horizontal plane (Figure 1) is:

$$\eta = \frac{\int \dot{m} c_p \left(T_1 - T_0\right) dt}{\int I A_c dt} = 0.65 \quad (3)$$

2.3. Thermogravimetric Analyzer

A thermogravimetric analyzer TGA Q500 from TA Instruments is used to obtain the drying kinetics of Granny Smith apples at isothermal conditions, and to reproduce the temperature profile (T_1) shown in Figure 3. The inert gas employed was nitrogen, flowing through the furnace at a rate of 0.06 l/min. The TGA weighting precision is ±0.01% and its sensitivity in the mass measurement is 0.1 μg. The apple samples employed in the tests where cylinders of 1 cm in diameter and a thickness of 2.4 mm. The mass of the Granny Smith apples used in the TGA measurements is around 150 mg. Even though the apple samples do not become oxidized in a nitrogen stream, the samples were immersed in citric acid to present the same initial conditions as those of the tests in the solar dryer. For the determination of the drying kinetics, tests at temperatures ranging from 20 °C to 50 °C, using intervals of 5 °C, were conducted, covering the whole operating range shown in Figure 3.

3. Mathematical model of the thin-layer drying process of Granny Smith apples

In this section, the drying curve for Granny Smith apples was estimated using thin-layer drying equations for a range of temperature from 20 °C to 50 °C, a typical drying temperature range for solar dryers. Based on these results, a mathematical model capable of predicting the evolution of the drying process for variable air temperatures is proposed.

3.1. Thin-layer drying equations

The drying process of biological products is governed by the diffusion mechanism of moisture during the falling rate period [28]. There are many equations available in the literature capable of predicting the evolution of the mass of the sample during the falling rate period of the drying process. The drying process is characterized by the moisture ratio, *MR*, a dimensionless parameter that quantifies the reduction of the moisture content of the sample with time [12, 20, 28]. The moisture ratio is defined as:

$$MR = \frac{M(t) - M_e}{M_0 - M_e} \tag{4}$$

where $M(t)$ is the moisture content (wet basis) after a time t, M_e is the equilibrium moisture content and M_0 is the initial moisture content. The moisture ratio *MR* varies between $MR = 1$, at the beginning of the drying process, and $MR = 0$, once the sample is dried at equilibrium with the drying air.

Different equations based on the thin-layer drying models available in the literature were used to model the evolution with time of the moisture ratio of Granny Smith apples dried at a constant temperature of 35 °C. The moisture loss was determined using the TGA and the moisture ratio was calculated using Eq. 4. The results were fitted to eleven different thin-layer drying equations. For the fitting procedure, the moisture ratio considered is between $MR = 1$ and $MR = 0.1$, since after that value, the drying rate decreases drastically and thus the samples are almost dry. Table 1 shows the equations proposed by different authors for the prediction of the moisture ratio during time, together with the values of the fitting parameters of each

equation obtained for the experimental results. The determination coefficient R^2 of the different fittings is also reported in the table.

Table 1: Fitting parameters of different thin-layer drying equations available in the literature applied to the moisture ratio obtained drying Granny Smith samples in TGA at 35 °C. Valid for $1 \geq MR \geq 0.1$.

Equation	Model name	Parameters	R^2 [-]	Reference
$MR = 1 + a \cdot t + b \cdot t^2$	Wang and Singh	$a = -0.00794\ min^{-1}$ $b = 1.28 \cdot 10^{-5}\ min^{-2}$	0.9999	[29]
$MR = \exp(-k \cdot t)$	Lewis	$k = 0.01074\ min^{-1}$	0.9865	[30]
$MR = \exp(-k \cdot t^n)$	Page	$k = 0.00257\ min^{-n}$ $n = 1.32$	0.9961	[31]
$MR = a \cdot \exp(-k \cdot t)$	Henderson and Pabis	$a = 1.078$ $k = 0.0118\ min^{-1}$	0.9798	[32]
$MR = a \cdot \exp(-k \cdot t)+c$	Logarithmic	$a = 1.888$ $k = 0.00441\ min^{-1}$ $c = -0.880$	0.9998	[18]
$MR = a \cdot \exp(-k_1 \cdot t)+b \cdot \exp(-k_2 \cdot t)$	Two terms	$a = 29.82$ $k_1 = 0.00255\ min^{-1}$ $b = -28.82$ $k_2 = 0.00236\ min^{-1}$	0.9999	[33]
$MR = a \cdot \exp(-k \cdot t)+(1-a) \cdot \exp(-k \cdot a \cdot t)$	Two terms exponential	$a = 1.846$ $k = 0.01629\ min^{-1}$	0.9952	[34]
$MR = a \cdot \exp(-k \cdot t)+(1-a) \cdot \exp(-k \cdot b \cdot t)$	Diffusion approximation	$a = -8.39$ $k = 0.01794\ min^{-1}$ $b = 0.9435$	0.9879	[35]
$MR = a \cdot \exp(-k_1 \cdot t)+(1-a) \cdot \exp(-k_2 \cdot t)$	Verma	$a = 4.823$ $k_1 = 0.00295\ min^{-1}$ $k_2 = 0.0016\ min^{-1}$	0.9998	[36]
$MR = a \cdot \exp(-k_1 \cdot t)+b \cdot \exp(-k_2 \cdot t)+c \cdot \exp(-k_3 \cdot t)$	Modified Henderson and Pabis	$a = -4.674$ $k_1 = 0.0339\ min^{-1}$ $b = 1.678$ $k_2 = 0.0509\ min^{-1}$ $c = 4.015$ $k_3 = 0.0215\ min^{-1}$	0.9989	[37]
$MR = a \cdot \exp(-k \cdot t^n)+b \cdot t$	Midilli	$a = 0.993$ $k = 0.00414\ min^{-n}$ $n = 1.13$ $b = -0.00135\ min^{-1}$	>0.9999	[38]

Based on the results shown in Table 1, and considering simplicity and accuracy criteria, the equation selected for the prediction of the moisture ratio is that proposed by Wang and Singh [29], which is a quadratic equation in the form:

$$MR = 1 + at + bt^2 \quad (5)$$

The moisture ratio as a function of time obtained in the TGA for the isothermal process at 35 °C is plotted in Figure 4 together with the fitting of Wang and Singh equation. The equation proposed by Wang and Singh described precisely the drying process occurring in the TGA at the temperature of 35 °C for moisture ratios above MR = 0.1, nevertheless the model is not capable of predicting properly the drying process for moisture ratios below 0.1.

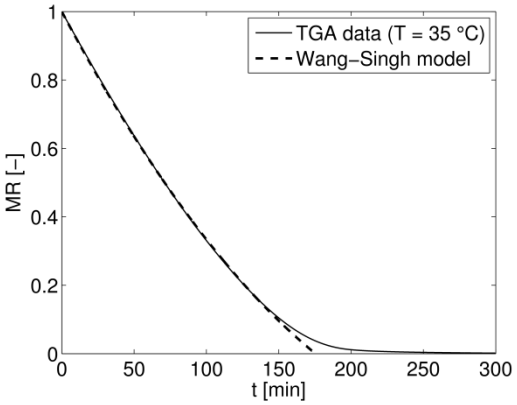

Figure 4: Moisture ratio obtained by the TGA at 35 °C and Wang and Singh equation fitting for the moisture ratio above *MR* = 0.1.

Several drying processes of Granny Smith apples were conducted in the thermogravimetric analyzer for constant temperatures ranging from 20 to 50 °C, using temperature intervals of 5 °C. Figure 5 shows the evolution of the moisture ratio (*MR*) with time (*t*) for the different constant temperatures tested. The tendency of the moisture ratio is similar for all the temperatures studied, but there is a strong effect of the temperature on the drying time (t_d).

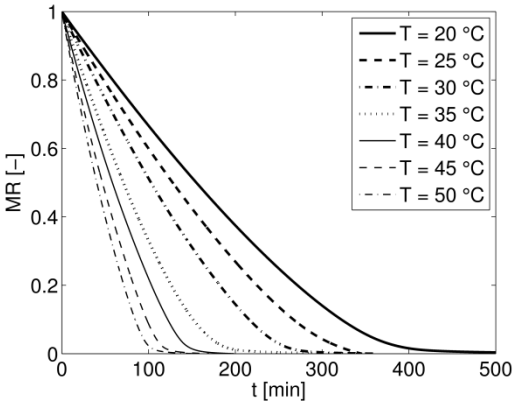

Figure 5: Evolution of the moisture ratio with time during the thin-layer drying of Granny Smith apples in TGA.

3.2. Mathematical model of the thin-layer drying process of Granny Smith apples at variable temperature

Following the procedure describe in Section 3.1, the equation proposed by Wang and Singh [29] (Eq. 5) was employed to fit the evolution of the experimental moisture ratio with time from *MR* = 1 to *MR* = 0.1, for each temperature. The values of the free parameters *a* and *b* in Eq. 2 obtained for each temperature are shown in Figure 6 a) and b) respectively, as a function of the constant temperature employed during the drying process in the TGA. The values

obtained for *a* and *b* are plotted in Figure 6 together with a parabolic fitting, showing a proper agreement of the fitting to the values. The determination coefficients of the fitting are R^2 = 0.997 for *a* and R^2 = 0.998 for *b*. The equations of the parabolic fitting for the parameters of the equation proposed by Wang and Singh [29] for the temporal evolution of the moisture ratio are:

$$a = -3.44 \cdot 10^{-6} T^2 - 1.35 \cdot 10^{-4} T + 1.26 \cdot 10^{-3} \quad (6)$$

$$b = 3.75 \cdot 10^{-8} T^2 - 1.39 \cdot 10^{-6} T + 1.44 \cdot 10^{-5} \quad (6)$$

where *a* is obtained in min^{-1} and *b* in min^{-2} for a temperature *T* in °C.

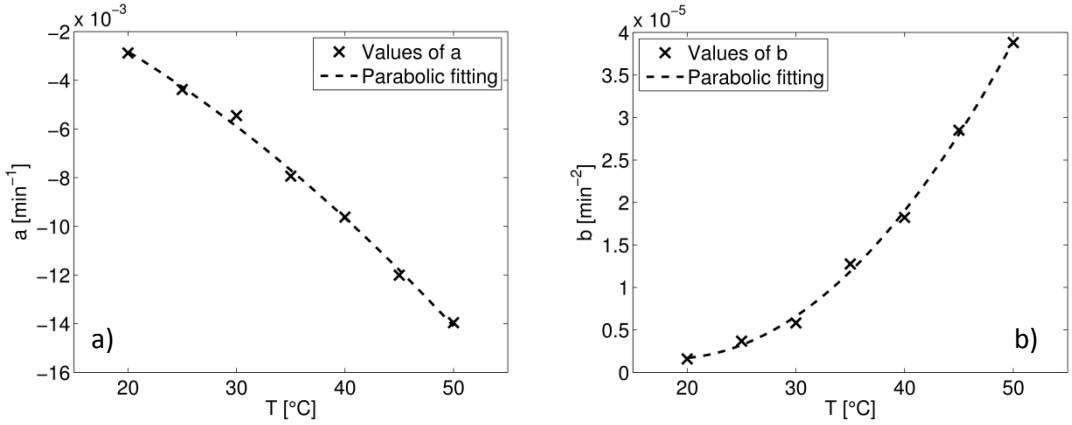

Figure 6: Values of the free parameters of the equation proposed by Wang and Singh [29] for the TGA measurements.

The values of *a* and *b* can be obtained for any temperature using respectively Eq. 6 and Eq. 7. Hence a model is proposed to estimate the evolution of the moisture ratio during the thin-layer drying process of Granny Smith apples conducted in a TGA under a variable temperature profile. The model considers a quasi-steady drying process where the thermal inertia of the sample is negligible. This assumption can be justified by the reduced size of the samples employed in the TGA tests (mass sample under 150 mg). The time is discretized in small time intervals (*dt*) of 10 ms, and for each time ($t = n \cdot dt$) the temperature is calculated. Using Eq. 6 and Eq. 7 the values of *a* and *b* are determined for the calculated temperature. Knowing the value of *MR* estimated by the model at the beginning of the time interval, the values of *a* and *b* obtained are employed to determine the decrement of the moisture ratio (ΔMR) for the time interval *dt*, considering the temperature constant during that short time period. Therefore, the value of the moisture ratio at the end of the time interval *dt* is calculated as the value at the beginning of the time interval minus the decrement of the moisture ratio, i.e. $MR(t + dt) = MR(t) - \Delta MR$. The initial condition for the moisture ratio, at the beginning of the drying process, is $t = 0\ s \rightarrow MR = 1$. The model estimates the evolution of the moisture ratio with time for $MR \geq 0.1$.

4. Results and discussion

4.1. Validation of the thin-layer drying model

The model proposed for the thin-layer drying of Granny Smith apples at a variable temperature was validated conducting a drying test in the TGA for variable drying temperatures. In order to employ a realistic drying temperature, the temperature measured at the inlet of the drying chamber in the lab-scale indirect solar dryer (Figure 3) was used to program the temperature profile in the TGA. The temperature at the inlet of the drying chamber was obtained using the operating conditions discussed in Section 2. Since the TGA Q 500 employed permits only to program constant heating rates, i.e. linear temperature increases, the temperature measured at the inlet of the drying chamber, shown in Figure 3, was divided into 30 linear temperature increases, which were programmed in the TGA. Since the temperature in the TGA cannot be controlled accurately during the cooling process, the test in the TGA ends once the maximum temperature is reached, that is after around 300 min. Nevertheless, the apple sample is totally dried ($MR \rightarrow 0$) before 300 min.

The model proposed in Section 3.2 was applied to the thin-layer drying process of the Granny Smith apple samples in the TGA, subjected to the temperature profile showed in Figure 3. The experimental value of the moisture ratio obtained in the TGA (MR_{TGA}) together with its experimental uncertainty, and the estimated value obtained from the model proposed (MR_{mod}) can be observed in Figure 7 a). The experimental uncertainty of the measurement of the moisture ratio in the TGA (shown in grey in Figure 7 a)) is reduced due to the high precision in the mass measurement. As can be seen in Figure 7 a), the model follows the trend of the evolution of the moisture ratio of the apples for a drying process with a variable temperature. In fact, the deviation between the model estimation of the drying time (t_d) and the experimental values is lower than 2.5 min for moisture ratios between 1 and 0.1, as shown in Figure 7 b). This maximum deviation of 2.5 min corresponds to a maximum relative error of the time estimated by the model of 1.5%. Nevertheless, the estimation of the moisture ratio performed by the model is inside the low range of uncertainty of the measurement of the TGA. Therefore, the model was proved to predict accurately the evolution of the moisture ratio during a variable temperature thin-layer drying process of Granny Smith apples."

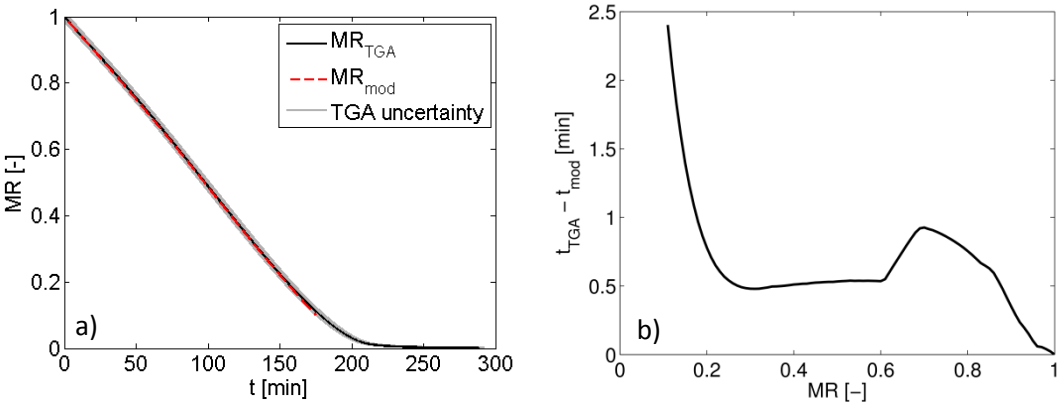

Figure 7: a) Measured and estimated evolution of the moisture ratio with time for the variable temperature drying process in the TGA, b) deviation between the estimated and the measured drying time.

4.2. Application of the drying model in an indirect solar dryer

Once validated using TGA measurements, the model was applied to the drying of Granny Smith apples in a solar indirect dryer. In this case, a total mass of around 80 g of slices of apples (2.4 mm in thickness) were dried on the reference tray in the drying chamber. The variation of the sample mass with time was measured with the balance each 5 s. Therefore, the evolution of the moisture ratio with time during the drying process in the indirect solar dryer can be calculated, and a procedure similar to that employed previously for the TGA measurements can be followed. First, several constant temperature drying tests were performed in the indirect solar dryer, using temperatures between 25 °C and 40 °C in intervals of 5 °C. In this case, for each value of the temperature, the corresponding value of the relative humidity of air was employed, following the weather data for the reference climate and the drying conditions explained in Section 2. The evolution with time of the moisture ratio obtained in the solar dryer for each temperature is plotted in Figure 8. An increase in the constant temperature of the drying process decreases significantly the drying time, similar to what was shown for the TGA experiments.

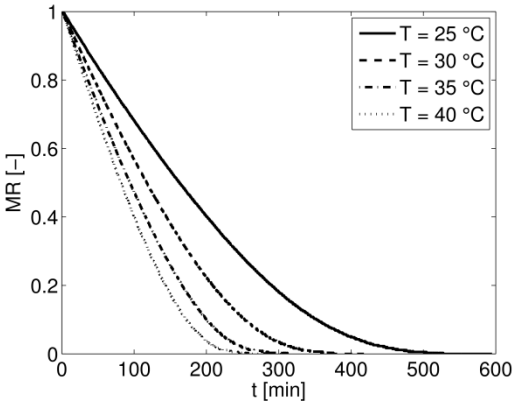

Figure 8: Evolution of the moisture ratio with time during the thin-layer drying of Granny Smith apples in an indirect solar dryer.

The moisture ratio curves obtained for each constant temperature in the indirect solar dryer were fitted to a curve as that proposed by Wang and Singh [29], shown in Eq. 5, determining the fitting parameters *a* and *b*. The values of the fitting parameters obtained for each temperature are presented in Figure 9, together with their parabolic fitting. The equations of the parabolic fitting of the parameters *a* and *b* of the Wang-Singh equation for the thin-layer drying of Granny Smith apples in the solar indirect dryer, considering the drying conditions explained in Section 2, are:

$$a_{SD} = 4.86 \cdot 10^{-6} T^2 - 5.38 \cdot 10^{-4} T + 6.93 \cdot 10^{-3} \quad (8)$$

$$b_{SD} = -5.87 \cdot 10^{-9} T^2 + 7.94 \cdot 10^{-7} T - 1.37 \cdot 10^{-5} \quad (9)$$

where a_{SD} is obtained in min^{-1} and b_{SD} in min^{-2} for a temperature *T* in °C.

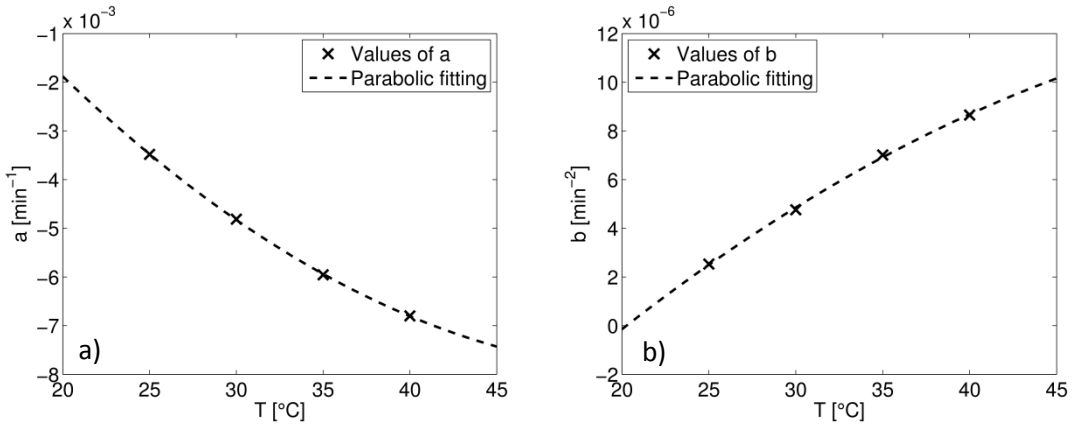

Figure 9: Values of the parameters of the equation proposed by Wang and Singh [29] for the indirect solar dryer measurements.

The model proposed for the thin-layer drying of Granny Smith apples at variable temperature was applied to the drying process in the solar indirect dryer. To that end, the values of the parameters a_{SD} and b_{SD} of the Wang-Singh equation for the solar dryer were obtained from Eq. 8 and Eq. 9 for each drying chamber temperature. The drying chamber temperature was that showed in Figure 3. Then, using the variable temperature and the parabolic fittings of the parameters a_{SD} and b_{SD} for the solar dryer, the proposed model can be employed to estimate the evolution of the moisture ratio with time during the thin-layer drying of Granny Smith apples. The values measured in the indirect solar dryer for the moisture ratio are shown in Figure 10 a), together with their uncertainty and the estimation of the model. The experimental curve showed in Figure 10 a) is the average of 4 different tests. Nevertheless, the tests present high repeatability, being the maximum deviation in the whole *MR* curve less than 0.01. In each test, 9 slices of apple where dried in the reference mesh detailed in section 2.2. In this case, the uncertainty associated to the measurement of the moisture ratio is higher than in the TGA, as a consequence of the lower weighing precision of the indirect solar dryer.

The model seems to overestimate the drying capacity of the solar indirect dryer, predicting lower drying times than those measured, falling even out of the uncertainty range of the experimental measurement for low values of the moisture ratio. The maximum deviation between the predicted and the measured drying time for the indirect solar dryer was lower than 20 min, as shown in Figure 10 b), corresponding to a maximum relative error around 10%. The higher error obtained for the estimations of the model for the drying process occurring in the indirect solar dryer might be attributed to the effect of the thermal inertia of the sample. For the experiments in the indirect solar dryer, the mass of the sample is much larger than the mass used in the TGA tests (approximately 80 g in the indirect solar dryer and just around 150 mg in the TGA), thus the temperature of the sample might differ from that measured in the air of the drying chamber. The lower temperature of the sample in the indirect solar dryer tests due to thermal inertia would delay the drying process, producing the differences observed in Figure 10.

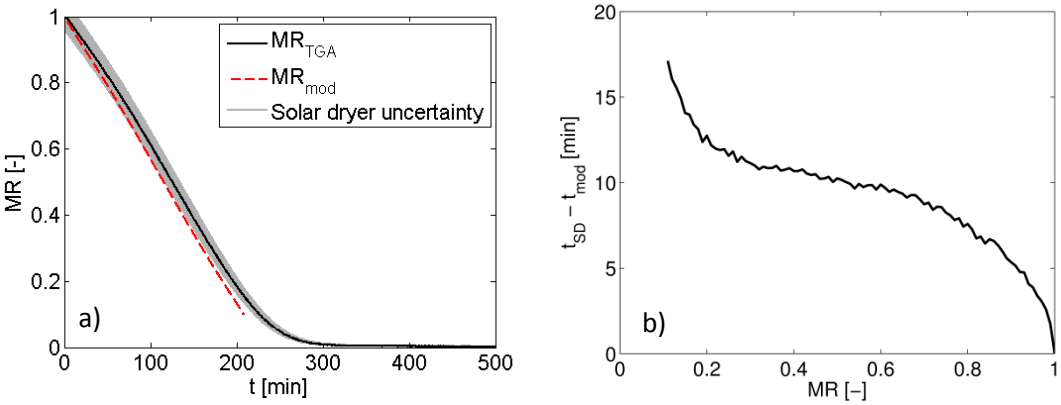

Figure 10: a) Measured and estimated evolution of the moisture ratio with time for the variable temperature drying process in the indirect solar dryer, b) deviation between the estimated and the measured drying time.

The effect of the thermal inertia of the sample on the delay of the drying process in the indirect solar dryer was analyzed performing drying tests using the atmospheric conditions described in Section 2 for various air mass flow rates. The nominal air mass flow rate of 0.015 kg/s was increased to 0.020 and 0.025 kg/s and drying tests were carried out. The process to obtain the estimations of the model proposed for the moisture ratio evolution was repeated for these new values of the air mass flow rate, and the deviations in time between the experimental measurements and the model predictions were quantified. The results are shown in Figure 11, where the time deviations for the three different air mass flow rates employed are plotted. The deviations are proved to decrease for higher air mass flow rates, as a consequence of the higher convection coefficient obtained using a higher air velocity, which reduces the effect of thermal inertia of the sample. In fact, the estimation of the model for the moisture ratio using an air mass flow rate of 0.025 kg/s falls inside the uncertainty associated to the experimental measurement.

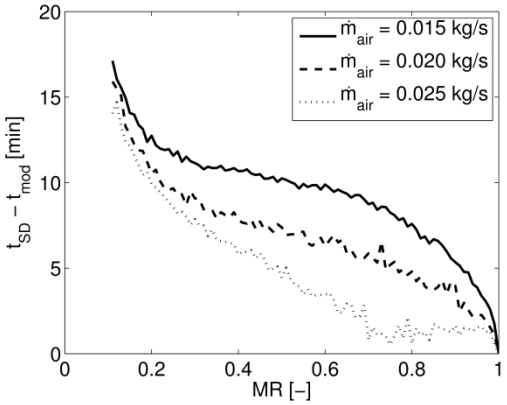

Figure 11: Deviation between the estimated and the measured drying time for different values of the air mass flow rate.

5. Conclusions

The kinetics of the thin-layer drying process of Granny Smith apples was experimentally analysed by means of thermogravimetric measurements. Drying tests were conducted at different constant drying temperatures in a TGA, obtaining the drying curves of Granny Smith

apples as a function of temperature. The Wang-Singh equation was employed to fit the experimental drying curves obtained in the TGA for constant temperatures. A novel model was proposed, based on the Wang-Singh equation, to predict the evolution of the moisture ratio during the thin-layer drying process of Granny Smith apples under variable temperature profiles. The model was validated using experimental results of the drying of apples in the TGA for a variable drying temperature. The prediction of the model proposed for the evolution of the moisture ratio with variable temperature was in excellent agreement with the experimental measurements obtained in the TGA, obtaining a maximum deviation from the experiments of 1.5%, a deviation which is inside the uncertainty associated with the measurements.

The model was also applied to the drying process of thin slices of Granny Smith apples in an indirect solar dryer. The procedure was replicated, obtaining the parameters of the Wang-Singh equation for the drying conditions presented in the solar drying process. The comparison of the model estimations with experimental measurements carried out in a lab-scale indirect solar dryer shows a proper agreement, obtaining deviations under 10%. Nevertheless, the experimental values of the moisture ratio were delayed compared to the model predictions, a result that can be attributed to the effect of the thermal inertia of the sample in the indirect solar dryer. This effect was proved increasing the air mass flow rate, obtaining in this case a prediction of the moisture rate from the model that falls inside the uncertainty range associated with the experimental measurement.

Acknowledgements

The thermogravimetric analyses were conducted in the BIOLAB experimental facility (madrimasd.org, lab # 202), a laboratory financed under the infrastructures and lab network of the Madrid (Spain) Regional Government.

Nomenclature

A_c– Solar collector area [m^2].

a– Free parameter in the Wang-Singh equation [s^{-1}].

b– Free parameter in the Wang-Singh equation [s^{-2}].

c_p – Specific heat of the air [J kg^{-1} K^{-1}]

dt – Time interval [s].

I – Solar irradiance on the horizontal plane [W m^{-2}].

I_T – Solar irradiance on the collector angle [W m^{-2}].

$\dot{m}_{air}$ – Air mass flow rate [kg s^{-1}].

M – Moisture content as a function of time (wet basis) [kg kg^{-1}].

M_e – Equilibrium moisture content (wet basis) [kg kg^{-1}].

M_0 – Initial moisture content (wet basis) [kg kg^{-1}].

MR – Moisture ratio [-].

R_b – Ratio of beam irradiance on tilted surface to that on the horizontal plane [-].

S – Solar irradiance absorbed by the absorber plate [W m^{-2}].

T – Temperature [°C].

t – Time [s].

t_d – Drying time [s].

Greek letters

β – Angle of inclination of the solar collector [°].

ΔMR – Moisture ratio reduction [-].

ρ_g – Ground reflectance [-]

$(\tau\alpha)$ – Effective transmittance-absorptance product [-].

ϕ – Relative humidity [-].

Subscripts

0 – Inlet of the collector

1 – Outlet of the collector, inlet of the drying chamber

b – Beam component

d – Diffuse component

g – Ground reflection

mod – Model

SD – Solar dryer

TGA – Thermogravimetric analyzer

References

[1] Kumar, M., Sansaniwal, M.K, Khatak, P., Progress in solar dryers for drying various commodities. Renewable and Sustainable Energy Reviews, 2016, 55, 346-360.

[2] Fudholi, A., Sopian, K., Ruslan, M.H., Alghoul, M.A., Sulaiman, M.Y. Review of solar dryers for agricultural and marine products. Renewable and Sustainable Energy Reviews, 2010, 14, 1-30.

[3] Gulcimen F., Karakaya H., Durmus A. Drying of sweet basil with solar air collectors, Renewable Energy, 2016, 93, 77-86.

[4] Velic, D., Planinic, M., Tomas, S., Bilic, M. Influence of airflow velocity on kinetics of convection apple drying. Journal of Food Engineering, 2004, 64, 97-102.

[5] Vega-Gálvez, A., Ah-Hen, K., Chacana, M., Vergara, J., Martínez-Monzó, J., García-Segovia, P., Lemus-Mondaca, R., Di Scala, K. Effect of temperature and air velocity on drying kinetics, antioxidant capacity, total phenolic content, colour, texture and microstructure of apple. Food Chemistry, 2012, 132, 51-59.

[6] Romano, G., Kocsis, L., Farkas, I. Analysis of energy and environmental parameters during solar cabinet drying of apple and carrot. Drying Technology, 2009, 27, 574-579.

[7] Lamnatoua, C., Papanicolaou, E., Belessiotis, V., Kyriakis, N. Experimental investigation and thermodynamic performance analysis of a solar dryer using an evacuated-tube air collector. Applied Energy, 2012, 94, 232-243.

[8] Elicin, A.K., Sacilik K. An experimental study for solar tunnel drying of apple. Tarim Bilimleri, 2005, 11(2), 207-211.

[9] Blanco-Cano, L., Soria-Verdugo, A., Garcia-Gutierrez, L.M., Ruiz-Rivas, U. Evaluation of the maximum evaporation rate in small-scale indirect solar dryers. ASME Journal of Solar Energy Engineering, 2016, 138, 0245021-0245024.

[10] Akpinar, E.K., Yasar, B. Modelling of the drying of eggplants in thin-layers. International Journal of Food Science and Technology, 2005, 40, 273–281.

[11] Zhu, A., Shen, X. The model and mass transfer characteristics of convection drying of peach slices. International Journal of Heat and Mass Transfer, 2014, 72, 345-351.

[12] Doymaz, I. An experimental study on drying of green apples. Drying Technology, 2009, 27, 478-485.

[13] Celma, A.R., Rojas, S., López, F., Montero, I., Miranda, T. Thin-layer drying behaviour of sludge of olive oil extraction. Journal of Food Engineering, 2007, 80 (4), 1261-271.

[14] Basunia, M.A., Abe, T. Thin-layer solar drying characteristics of rough rice under natural convection. Journal of Food Engineering, 2001, 47, 295-301.

[15] Aktaş M., Ceylan I., Yilmaz S. Determination of drying characteristics of apples in a heat pump and solar dryer. Desalination, 2009, 239 (1-3), 266-275.

[16] Janjai, S., Lamlert, N., Intawee, P., Mahayothee, B., Bala, B.K., NagleM., Muller, J. Experimental and simulated performance of a PV-ventilated solar greenhouse dryer for drying of peeled longan and banana, Solar Energy, 2009, 83, 1550-1565.

[17] Karim, M.A., Hawlader, M.N.A. Drying characteristics of banana: theoretical modelling and experimental validation. Journal of Food Engineering, 2005, 70, 35-45.

[18] Sacilik, K., Elicin, A.K. The thin layer drying characteristics of organic apple slices. Journal of Food Engineering, 2006, 73, 281-289.

[19] Menges, H.O., Ertekin, C. Mathematical modelling of thin layer drying of Golden apples. Journal of Food Engineering, 2006, 77, 119-125.

[20] Zlatanovic, I., Komatina, M., Antonijevic, D. Low-temperature convective drying of apple cubes. Applied Thermal Engineering, 2013, 53, 114-123.

[21] Sturm B., Nunez Vega A.M., Hofacker, W. C. Influence of process control strategies on drying kinetics, colour and shrinkage of air dried apples, Applied Thermal Engineering, 2014, 62 (2), 455-460.

[22] Velic, D., Bilic, M., Tomas, S., Planinic, M., Bucic-Kojic, A., Aladic, K. Study of the drying kinetics of "Granny Smith" apple in tray drier. Agriculturae Conspectus Scientificus, 2007, 72 (4), 323-328.

[23] González-Fésler, M., Salvatori, D., Gómez, P., Alzamora, S.M. Convective air drying of apples as affected by blanching and calcium impregnation. Journal of Food Engineering, 2008, 87, 323-332.

[24] Iglesias, I., Carbó, J., Bonany, J., Montserrat, R. Varietal innovation in apples. Revista de Fruticultura, 2009, 1 (10), 13-25.

[25] Energy Plus. Weather Data. https://energyplus.net/weather Last access: Feb 2016.

[26] Duffie, J.A., Beckman, W.A. Solar Engineering of Thermal Processes. John Wiley and Sons. Hoboken, New Jersey, 2006. Third Edition.

[27] Ekechukwu, O.V., Norton, B. Review of solar-energy drying systems III: low temperature air-heating solar collectors for crop drying applications. Energy Conversion and Management, 1999, 4, 657-667.

[28] Panchariya P.C., Popovic, D., Sharma, A.L. Thin-layer modelling of black tea drying process. Journal of Food Engineering, 2002, 52, 349-357.

[29] Wang, C.Y., and Singh, R.P. A single layer drying equation for rough rice. ASAE, 1978, paper No: 78-3001, ASAE, St. Joseph, MI.

[30] Lewis, W.K. The Rate of Drying of Solid Materials. The Journal of Industrial and Engineering Chemistry, 1921, 13(5), 427-432.

[31] Page, G. Factors influencing the maximum rates of air drying shelled corn in layers. M. S. thesis, 1949, Purdue University.

[32] Henderson, S.M. and Pabis, S. Grain drying theory. I. Temperature effect on drying coefficient. Journal of Agricultural Engineering Research, 1961, 6(3), 169-174.

[33] Madamba, P.S., Driscoll, R.H., Buckle, K.A. The thin layer drying characteristics of garlic slices. Journal of Food Engineering, 1996, 29, 75-97.

514 [34] Ertekin, C., Yaldiz, O. Drying of eggplant and selection of a suitable thin layer drying model.
515 Journal of Food Engineering, 2004, 63, 349-359.

516 [35] Togrul, I.T., Pehlivan, D. Mathematical modeling of solar drying of apricots in thin layers.
517 Journal of Food Engineering, 2002, 55, 209-216.

518 [36] Verma, L.R., Bucklin, R.A., Endan, J.B., Wratten, F.T. Effects of drying air parameters on
519 rice drying models. Transactions of the ASAE, 1985, 28, 296-301.

520 [37] Karathanos, V.T. Determination of water content of dried fruits by drying kinetics. Journal
521 of Food Engineering, 1999, 39, 337-344.

522 [38] Midilli, A., Kucuk, H, Yapar, Z. A new model for single layer drying. Drying Technology,
523 2002, 20(7), 1503-1513.